Semiconductor-metal transition and the onset of itinerant ferromagnetism in the Heusler phases TiCoSn-TiCoSb

1995 J. Phys.: Condens. Matter 7 7373

(http://iopscience.iop.org/0953-8984/7/37/010)

J. Phys.: Condens. Matter 7 (1995) 7373–7385. Printed in the UK

Semiconductor–metal transition and the onset of itinerant ferromagnetism in the Heusler phases TiCoSn–TiCoSb

M A Kouacou†, J Pierre† and R V Skolozdra†‡

† Laboratoire L Néel, CNRS, 166X, 38042 Grenoble, France

‡ Department of Inorganic Chemistry, Y Franko University, 290005 Lviv, Ukraine

Received 7 April 1995, in final form 21 June 1995

Abstract. The magnetic and transport properties of the $TiCoSn_xSb_{1-x}$ solid solutions with the cubic MgAgAs structure have been studied, and show the onset of ferromagnetism associated with a semiconductor to metal transition, keeping the same 3d elements and varying the number of s–p electrons. The transition from TiCoSn ferromagnetic metal to the non-magnetic semiconductor TiCoSb occurs through an intermediate metallic Pauli-like state. The variations of the Curie temperature as a function of saturation and effective paramagnetic moments are related to the itinerant ferromagnetism model. A comparison is made with the $TiCo_xNi_{1-x}Sn$ series, where the transition occurs directly from ferromagnetic metal to semiconducting state.

1. Introduction

Cubic Heusler alloys are exemplary materials for the study of the magnetism of 3d metals, and many studies have been devoted to them. These cubic phases have the composition X_2YZ, where X and Y are transition metals, and Z is an sp element [1–4].

Manganese compounds X_2MnZ are examples of localized magnetism obtained from delocalized electrons [2, 3]. Conversely, Co_2YZ compounds exhibit a more itinerant magnetism [4, 5].

The 'semi-Heusler' phases with MgAgAs structure were studied more recently; they have the same cubic cell as true Heusler phases, but their composition is XY·Z, with a vacant site · replacing each second X atom [6]. As X atoms are more distant than in the previous structure, more localization of their magnetic shells can be expected.

We studied previously [7] the onset of itinerant ferromagnetism from a semiconducting state in the solid solution between TiCoSn and TiNiSn. TiCoSn orders ferromagnetically at 135 K with a saturation moment $M_f(0) = 0.35\ \mu_B$. Conversely, TiNiSn is a semiconductor with a small gap [8]. As Co is progressively replaced by Ni, the resistivity behaviour turns from metallic to semiconducting; the Co magnetism becomes more and more localized, without a large change in the effective magnetic moment of Co (from 1.35 μ_B in TiCoSn to 1.1 μ_B for Co diluted in TiNiSn).

Instead of filling the 3d band by the Co–Ni substitution, we may change the Fermi level by adding one electron on the sp site, replacing Sn by Sb. In the present work, we study the properties of the TiCoSn–TiCoSb series. TiCoSb, which has 18 peripheral electrons as does TiNiSn, is also a semiconductor as we shall see, with a small nearly constant susceptibility. The metal–semiconductor transition and the onset of magnetism can thus be studied in the series without changing the Co concentration.

0953-8984/95/377373+13$19.50

Magnetic measurements, resistivity, magnetoresistance and Hall effect experiments were performed; the variations of magnetic moments and interactions will be compared to those of the previously studied series and to the models for itinerant magnetism.

2. Preparation and crystallographic properties

The samples were prepared in polycrystalline form by melting constituents in an induction furnace under argon atmosphere. There were annealed during 7 to 30 days under high vacuum at 650 °C or 800 °C, in order to obtain a good crystallographic order. X-ray studies allowed us to identify the phases and to obtain the lattice parameters, which are given in table 1. For Sn-rich as well as for Sb-rich solutions, a unique cubic phase, with the reflections characteristic of ordered Heusler phases, was obtained.

Table 1. Lattice parameters for $TiCoSn_xSb_{1-x}$ solutions at 300 K. The mean standard deviation is 0.005 Å. Two phases occur in the middle of the series.

Compound	a (Å)	Compound	a (Å)
TiCoSn	5.997	$TiCoSn_{0.9}Sb_{0.1}$	5.988
$TiCoSn_{0.8}Sb_{0.2}$	5.967	$TiCoSn_{0.7}Sb_{0.3}$	5.940
$TiCoSn_{0.6}Sb_{0.4}$	5.920	$TiCoSn_{0.5}Sb_{0.5}$	5.906/5.946 (2 phases)
$TiCoSn_{0.4}Sb_{0.6}$	5.90/5.86 (2 phases)	$TiCoSn_{0.3}Sb_{0.7}$	5.892
$TiCoSn_{0.2}Sb_{0.8}$	5.886	$TiCoSn_{0.1}Sb_{0.9}$	5.880
TiCoSb	5.877		

However, two coexisting phases were observed in the middle of the series, for $0.35 < x(\mathrm{Sn}) < 0.6$, regardless of annealing time or temperature. Both phases belong to the Heusler structure, and have close-by lattice parameters. Thus some miscibility gap exists in the middle of the series; this feature must be kept in mind when analysing magnetic or transport data. It also shows that bonding is qualitatively different in the two limiting compounds.

3. Transport measurements

3.1. Resistivity and magnetoresistance

The resistivity was measured from 2 to 300 K using the four-probe method with AC current. Magnetoresistance and Hall effect measurements were performed on some compounds with fields up to 6 T.

Resistivity curves are drawn in figure 1 for Sn-rich samples ($1 < x(\mathrm{Sn}) < 0.4$), and in log–log scales in figure 2 which includes other semiconducting samples.

The resistivity for TiCoSb sample (the most resistive sample that we obtained) shows a semiconducting behaviour, reaching 1.5×10^5 $\mu\Omega$ cm at 2 K. Plotting $\log(R)$ as a function of $1/T$ allows us to deduce a gap of 55 meV from data taken between 120 and 300 K. This small value is probably not representative of the true gap (intrinsic activation energy) in the pure compound, as the gap reaches 0.4 eV in the TiNiSn isoelectronic compound [8]. Also the temperature dependence of the resistivity below 100 K is characteristic of extrinsic (impurity) conduction, which is quite normal for a ternary compound with vacancies. Most probably the observed gap represents the energy difference between donor levels and the conduction band edge, as the Hall effect (see below) indicates that negative carriers are

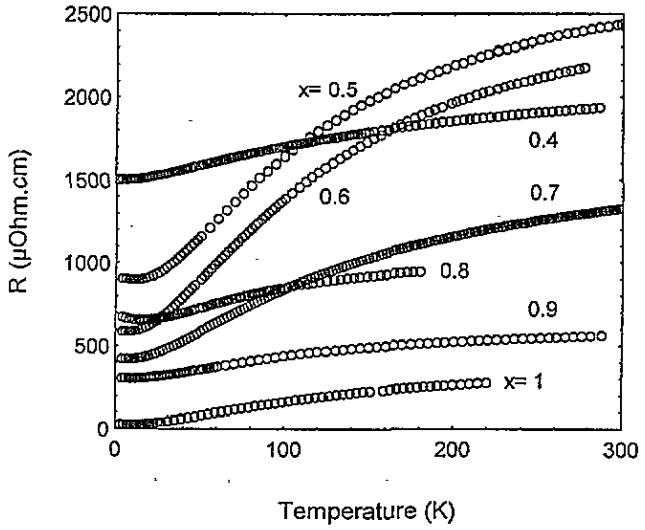

Figure 1. Resistivity versus temperature for metallic samples, x being the Sn proportion.

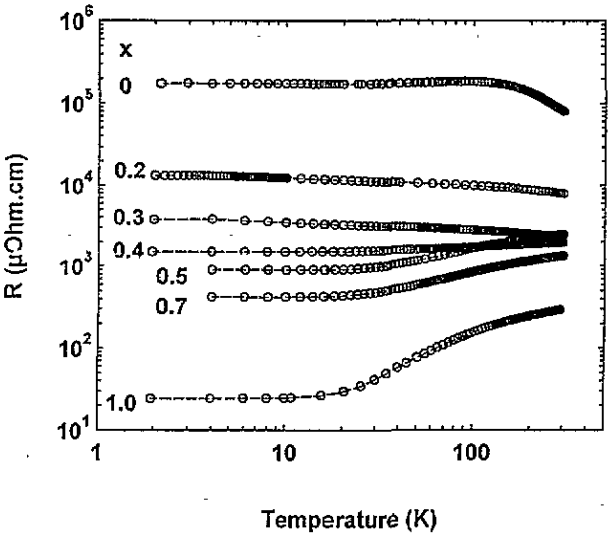

Figure 2. Resistivity versus temperature including some semiconducting samples.

dominant. These electron states may come from atomic disorder, as Co and Sn atoms may be present on the vacancy sites of the structure [7, 8]. It would be useful to extend transport measurements to higher temperatures in order to recover the true intrinsic regime.

When Sb is replaced by Sn, the resistivity decreases as expected for this heavy doping; the semiconducting behaviour disappears between $x(\mathrm{Sn}) = 0.3$ and $x = 0.4$, where the resistivity is nearly temperature independent with a value of about 2000 $\mu\Omega$ cm close to Mott's metallic limit. Between $x(\mathrm{Sn}) = 0.35$ and 0.6 (two-phase region), the data should be taken with caution, and interpreted as parallel transport shared by the two phases; one of them may be semiconducting while the other is metallic. Encouragingly, data seem

to behave regularly with the Sn concentration. For larger Sn concentration, a metallic behaviour is observed (figure 1), the low-temperature resistivity drops by a factor of 10^4 from TiCoSb to TiCoSn.

Table 2. Resistivity $\rho(0)$ at 0 K, A coefficient from the fits $\rho(T) = \rho(0) + AT^2$ at low temperature and $\rho(300\text{ K}) - \rho(0\text{ K})$.

x(Sn)	$\rho(0)$ ($\mu\Omega$ cm)	A (10^{-8} Ω cm K^{-2})	$\rho(300) - \rho(0)$ ($\mu\Omega$ cm)
1	22	1.22	255
0.9	299	2.38	262
0.8	656	3.33	289
0.7	412	7.30	912
0.6	570	14.12	1600
0.5	897	11.53	1539
0.4	1501	4.15	441

Within the metallic range, the resistivity behaves at low temperature as $\rho(0) + AT^2$, as in many spin fluctuation systems. The observed values for $\rho(0)$, A and $\rho(300) - \rho(0)$ are given in table 2. The A coefficient increases first with the Sb content, from 1.22×10^{-8} to 14.1×10^{-8} Ω cm K^{-2} and then drops down to smaller values before the metal to semiconductor crossover. As we shall see, this enhancement corresponds to the region where the magnetism disappears. For comparison, $ZrZn_2$ has an A coefficient equal to 4.7×10^{-8} Ω cm K^{-2} [9].

Magnetoresistance (MR) measurements have been performed for some compounds in the metallic range. TiCoSn [7] presents a strong positive MR at low temperatures. Sb substitution lowers the MR, which however remains strong and positive up to 40% Sb. This high value of the MR can be explained by a cyclotron-like contribution, but this contribution is certainly enhanced by the decoupling of the up and down subbands, as we are close to the upper edge of these bands.

3.2. *Hall effect and thermopower*

The Hall effect has been measured by the Van der Pauw method on square platelets for the two extreme compounds. For TiCoSb, it decreases from a nearly vanishing value at low temperature (as expected for a nearly compensated semiconductor) to the largest negative value of -1.5×10^{-7} Ω m T^{-1} near 200 K (figure 3). This indicates either that electrons are more mobile than holes (at high temperature), or rather that majority impurities are donor levels. The same behaviour was observed for TiNiSn, where electrons were found to be dominant carriers above 80 K [7, 8]. Aliev *et al* [8] quoted the influence of electron states due to atoms present on the vacancy sites; the high-temperature negative value in the intrinsic regime can be also explained by the respective curvature and degeneracy of the valency and conduction bands. It would be interesting to extract the Hall mobility and density of carriers from a comparison between resistivity and Hall effect, but in this case we have four independent variables which are hole and electron concentrations and mobilities, which cannot be obtained from the present data. The donor and acceptor concentrations also vary from sample to sample, which reduces the interest of the question. The Hall mobility $\mu = R_H^0/\rho$ given in figure 3 goes to zero at low temperature due to compensation and has no simple significance in this range.

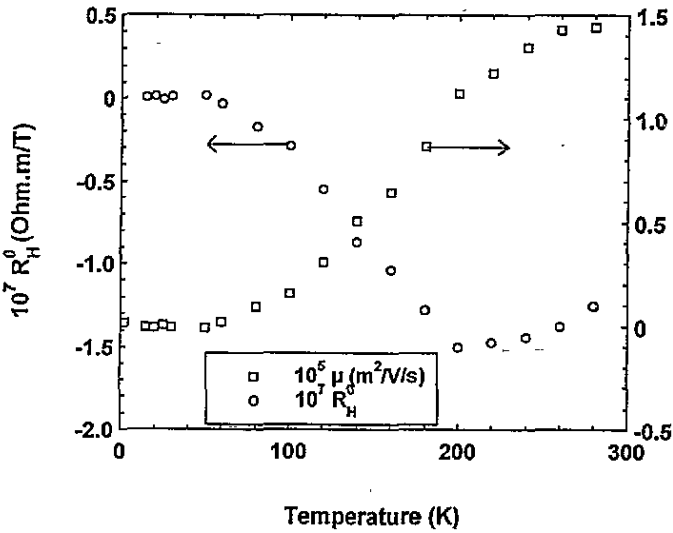

Figure 3. Temperature dependence of the (ordinary) Hall coefficient and the Hall mobility R_H^0/ρ for TiCoSb (see text).

Thermopower measurements were performed between 80 and 360 K. The Seebeck coefficient S is negative for TiCoSb (-50 μV K^{-1} at 350 K), which indicates in agreement with the Hall effect that negative carriers are dominant. When doping with Sn, S changes its sign near $x(\mathrm{Sn}) = 0.1$, and rises up to $+60$ μV K^{-1} for $x = 0.2$, which is expected as holes develop in the initial valency band. For higher Sn concentrations, S decreases and finally turns again negative in TiCoSn.

TiCoSn has also a negative ordinary Hall coefficient R_H^0 [7], but with a much smaller magnitude in agreement with its high carrier density. For ferromagnetic compounds, an anomalous Hall effect is related to the magnetization, the Hall resistivity being written as

$$V_H/I = \rho_H(B,T) = R_H^0 B + R_H^a M_f(B,T)$$

where V_H is the Hall voltage, B the induction, and R_H^a the anomalous Hall coefficient. This last coefficient is generally temperature dependent, and is related to the thermal dependence of the resistivity. Figure 4 represents the Hall resistivity behaviour as a function of field in the neighbourhood of the Curie point. One remarkable effect is that the spontaneous Hall effect $R_H^a M_f(0,T)$, which is the ordinate intercept at zero field, does not decrease to zero at the Curie point, as the static magnetization does, but remains until about 250 K (figure 5). Plotting the Hall resistivity as a function of the magnetization in this temperature range gives the same result.

This new feature can be explained in the following sense. For TiCoSn, as for other itinerant ferromagnets, strong spin correlations remain above the Curie point. The ferromagnetic clusters have a characteristic correlation length and fluctuation time, which increase with decreasing temperature and diverge at the Curie point. These ferromagnetic clusters have also a high susceptibility, which is revealed by the curvature of the reciprocal susceptibility above T_C, and thus are aligned rapidly by the magnetic field, although no spontaneous magnetization exists in zero field. Conduction electrons, which have a high velocity at the Fermi level, sense these ferromagnetic clusters as static, as their travelling time through these clusters is of the order of 10^{-12} s, much shorter than the fluctuation

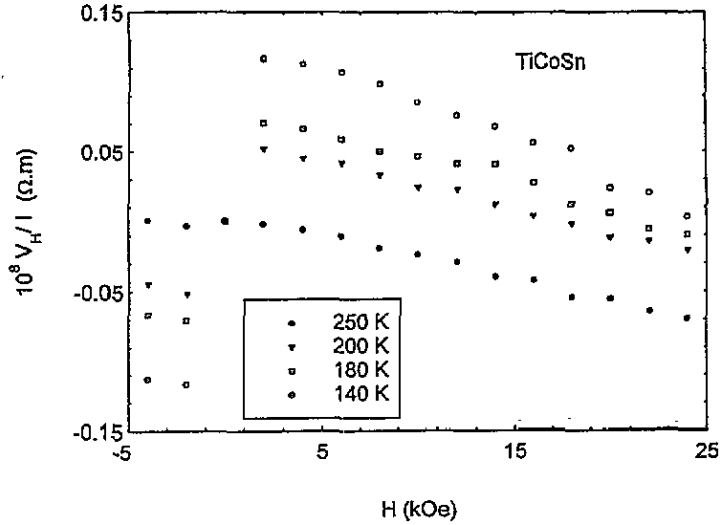

Figure 4. Hall resistivity as a function of applied field for TiCoSn in the vicinity of the Curie point (134 K).

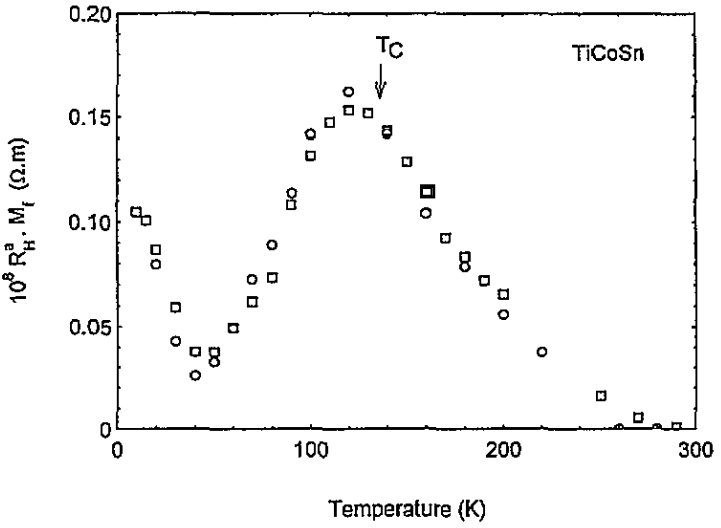

Figure 5. Temperature dependence of the spontaneous Hall effect in TiCoSn.

time. Thus they suffer a Hall-type deviation due to their magnetic interactions with the local magnetization, until the fluctuation time and/or the susceptibility are significantly reduced by increasing temperature.

4. Magnetic properties in the series

Magnetic measurements were performed in fields up to 9 T between 1.5 and 300 K. The spontaneous magnetization and the susceptibility in the paramagnetic range were

deduced from Arrott–Belov plots of M^2 versus H/M. For semiconducting systems, the magnetization curves are nearly linear and such a process is not necessary. In the following, the spontaneous magnetization obtained from the formula is denoted as M_f; the paramagnetic moment M_p is deduced from the Curie constant assuming the local moment relation $C_M = N\mu_B^2 M_p^2/3k_B$.

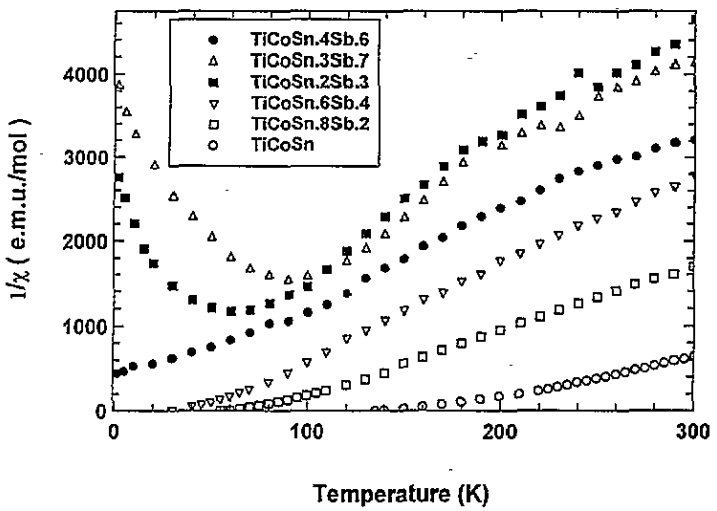

Figure 6. Reciprocal susceptibility for some solid solutions.

4.1. Paramagnetic susceptibility

The reciprocal susceptibility for some samples is given in figure 6. For the Sn-rich samples ($x > 0.5$), the solutions order ferromagnetically, and the susceptibility follows a Curie–Weiss law for temperatures well above the Curie point (typically for $T > T_C + 50$ K) (figure 6). As for previously studied Co–Ni compounds [5, 7], the reciprocal susceptibility has a non-linear behaviour and a positive curvature just above T_C, which is the common behaviour of itinerant ferromagnets [10]. The paramagnetic temperature Θ_p is thus higher than the ordering Curie point T_C (table 3).

For Sn concentration lower than 0.5, there is no more ferromagnetic order; the susceptibility does not follows the Curie–Weiss law; it tends to a finite value for $x(\mathrm{Sn}) = 0.4$, and for smaller Sn content it passes through a maximum value at a temperature which depends on composition (figure 6). This last behaviour is typical for numerous exchange-enhanced paramagnets, for instance YCo_2, $LuCo_2$ and related systems [11], and also for the $ZrZn_2$ weak ferromagnet when it turns paramagnetic under pressure [12].

Figure 7 shows the behaviour of paramagnetic moment M_p and ferromagnetic moment $M_f(0)$ in the series. It should be noted that the paramagnetic moment is nearly proportional to the Sn concentration. This behaviour is different from that found in the $TiCo_xNi_{1-x}Sn$ series [7], where the effective moment per Co atom was found to be nearly constant in spite of its localization.

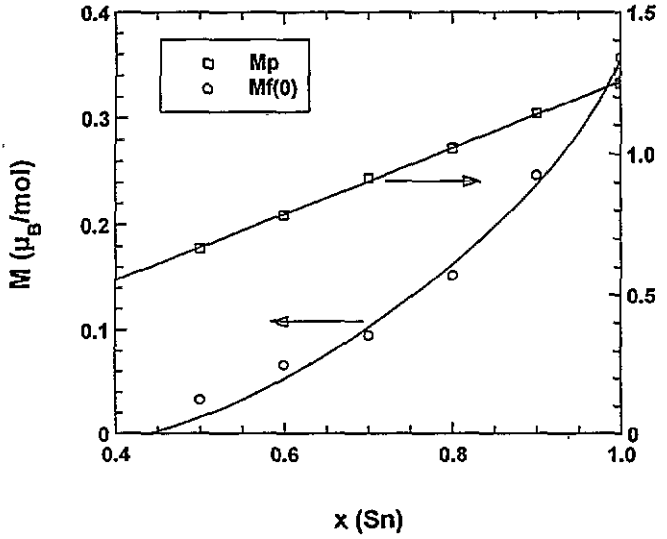

Figure 7. Variations of saturation ferromagnetic moment $M_f(0)$ and paramagnetic moment M_p as functions of Sn concentration.

Table 3. *Magnetic properties of* $TiCoSn_xSb_{1-x}$ *solid solutions. The moments and* susceptibilities are given per formula unit, susceptibilities in emu.

x(Sn)	Θ_p (K)	M_p (μ_B)	T_C (K)	$M_f(0)$ (μ_B)	$10^4\chi_0$	$10^4\chi_{max}$
1	176	1.25	134	0.357	—	—
0.9	130	1.14	101	0.246	—	—
0.8	78	1.02	52	0.152	—	—
0.7	65	0.915	35	0.095	—	—
0.6	49	0.785	28	0.066	—	—
0.5	38	0.667	17	0.033	—	—
0.4	—	—	—	—	20.0	—
0.3	—	—	—	—	3.32	8.58
0.2	—	—	—	—	2.81	6.50
0.1	—	—	—	—	1.54	2.74
0	—	—	—	—	1.0	2.20

4.2. Spontaneous magnetization and Curie temperature

A non-vanishing spontaneous magnetization is found for x(Sn) > 0.5. The saturation moment $M_f(0)$ found by extrapolating data to 0 K is given in figure 7 and table 3. For $x = 0.9$ and 0.8, the square of the magnetization $M_f^2(T)$ varies as $T^{4/3}$ (figure 8), this behaviour has been predicted by Moriya [13] and Lonzarich and Taillefer [14] for itinerant magnets close to the magnetic–non-magnetic limit. This law helps to determine the Curie temperature more precisely.

However, for $x = 0.7$, 0.6, 0.5, we find that $M_f(T)$ varies nearly linearly with temperature (figure 9). For the last compound, we observed two crystallographic phases, thus one explanation for the variation of the magnetization in this case may be that one phase may remain ferromagnetic when the other is paramagnetic, leading to a smearing of the ferromagnetic transition. The same kind of argument may hold also for other samples

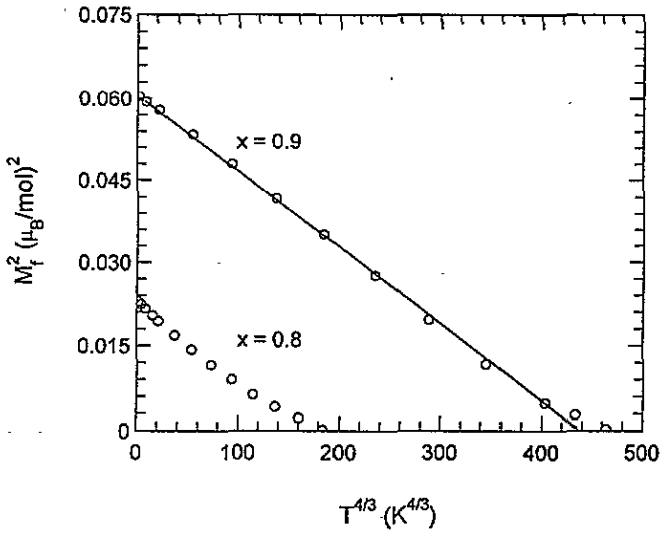

Figure 8. Variation of the square of spontaneous magnetization as a function of $T^{4/3}$ for x(Sn) = 0.9, 0.8.

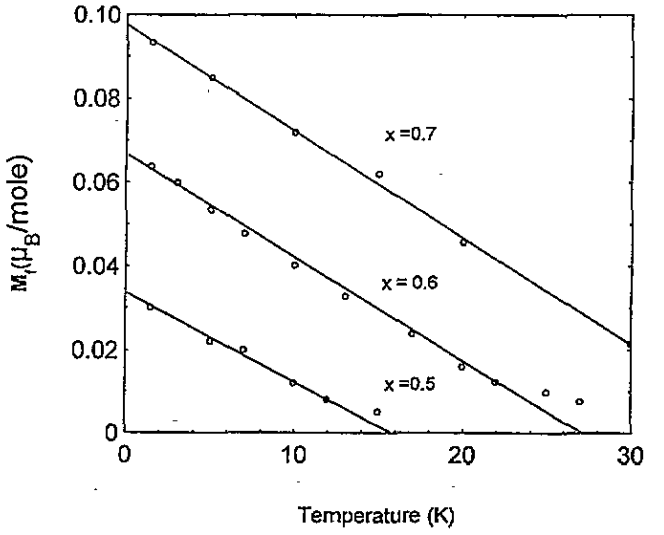

Figure 9. Temperature variation of spontaneous magnetization, x(Sn) = 0.7, 0.6, 0.5.

close to the ferromagnetic limit: the Co moment is very sensitive to its local environment, which varies from site to site due to the random replacement of Sn by Sb. Another, but a more dubious, explanation may be the strong drop in the density of states, as the Fermi level aproaches the band edge, which may modify substantially the thermal behaviour of the magnetization.

Finally, the Curie temperature varies nearly linearly with $M_f(0)$ (figure 10), whereas a quadratic law is expected for localized systems.

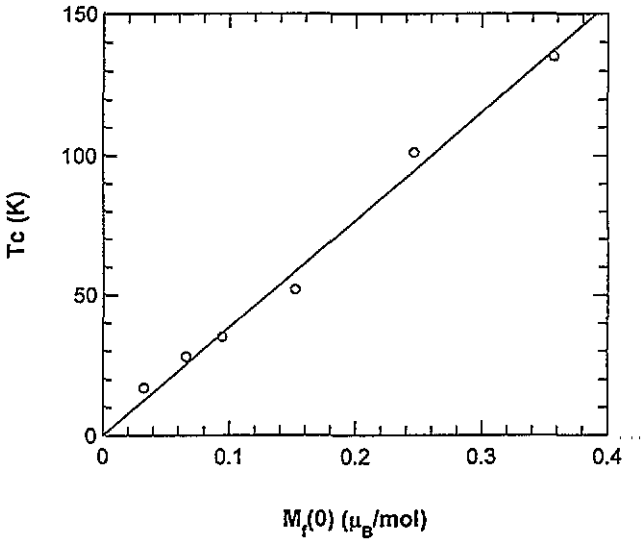

Figure 10. Variation of T_C as a function of saturation magnetization in the TiCoSn–TiCoSb series.

5. Discussion

In the present series, T_C, Θ_p, $M_f(0)$ and M_p decrease when the Sn concentration decreases. The variation of moments and interactions will be compared to those found in the $TiCo_xNi_{2-x}Sn$ series [5], where we pass from a Pauli paramagnet to a ferromagnetic metal, and to the $TiCo_xNi_{1-x}Sn$ series [7], where the solution turns directly from a semiconductor to a ferromagnetic metal as Co concentration increases.

The first point to discuss is whether or not the crossover from ferromagnetic metal to non-magnetic semiconductor occurs directly or through some intermediate Pauli paramagnetic phase. The disappearance of ferromagnetism occurs between $x = 0.5$ and $x = 0.4$, for a resistivity close to 2000 $\mu\Omega$ cm. The compound with $x = 0.4$ has still a resistivity increasing with temperature; however it is composed of two phases, thus we can only say that one of them at least is metallic and we cannot ascertain in this way that the magnetic–non-magnetic transition coincides with the metal–semiconductor (M–SC) transition.

One of the best tests of the nature of the magnetic–non-magnetic transition is probably the variation of T_C as a function of the saturation moment. For the $TiCo_xNi_{1-x}Sn$ series, we observed that T_C is roughly proportional to $M_f(0)^2$, whereas the effective paramagnetic moment per Co atom was found to be more or less constant. This is the general behaviour of localized systems, and indeed the Co moment localizes in this series without strong changes in magnitude when passing the M–SC transition. Conversely, in the $TiCo_xNi_{2-x}Sn$ metallic series, T_C is proportional to $M_f(0)^{1.05}$, a low power of the saturation moment which indicates that the interactions increase between decreasing moments. This behaviour is also found in heavy-fermion systems, accompanied by an enhancement of the specific heat coefficient and of the T^2 term in the low-temperature resistivity at the magnetic–non-magnetic crossover. In the case of the present series, the behaviours of the Curie temperature and of the resistivity coefficient seem to indicate that the ferromagnetic metal turns first to a Pauli paramagnetic metal before the M–SC transition takes place.

Let us note finally that independently of the nature of the transition, the $M_f(0)/M_p$ ratio increases with T_C, which is the general behaviour of itinerant magnets as described by the Rhodes–Wohlfarth theory [15]. T_C is proportional to $[M_f(0)/M_p]^{1.6}$ (figure 11), the variation being very close to that observed for the $TiCo_xNi_{1-x}Sn$ series. This fact underlines the well known universality of the Rhodes–Wohlfarth law for different concentrations and environments.

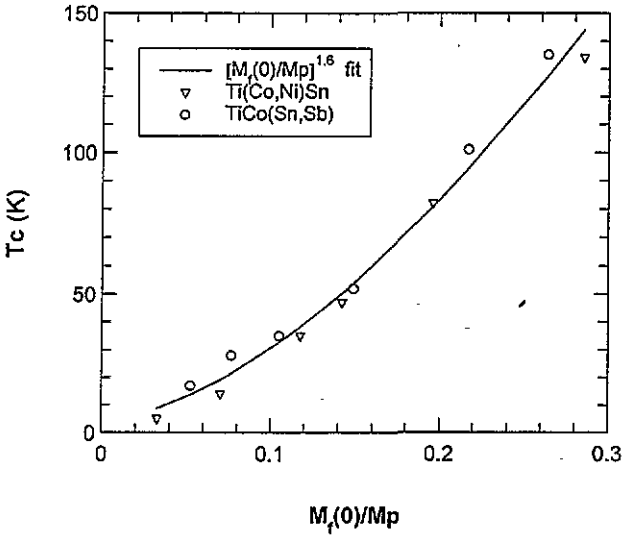

Figure 11. Variation of T_C as a function of $M_f(0)/M_p$ in the two series showing a metal–semiconductor crossover. The continuous line is a fit $T_C \sim [M_f(0)M_p]^{1.6}$.

A second point is the behaviour of the susceptibility for low Sn concentrations. As said previously, the susceptibility passes through a maximum in the temperature range between 50 and 100 K. This rounded maximum is not due to some antiferromagnetic order, but is related to the behaviour of exchange-enhanced paramagnets. The value for $\chi(0)$ decreases from 20×10^{-4} for $x = 0.4$ (close to ferromagnetism), to 1.0×10^{-4} emu mol^{-1} for TiCoSb where the susceptibility does not vary much with temperature. The values for intermediate concentrations are close to those found [11] for YCo_2, $LuCo_2$ (5.3×10^{-4} and 4.4×10^{-4} emu mol^{-1} respectively), the temperature for the maximum being also in the same range of magnitude. For $ZrZn_2$, Grosche *et al* [12] observed a transition from itinerant magnetism to enhanced paramagnetism under pressure, with a susceptibility behaviour which is quite similar to that found here by varying the concentration in the series.

One question arises about the behaviour of Co in TiCoSb, which is non-magnetic whereas Co keeps an effective moment of 1.1 μ_B when diluted in TiNiSn semiconductor [7]. The first naive explanation is that the Co 3d shell may be filled completely through an electron transfer from Sb. However, preliminary band calculations [16] show that the Co configuration in TiCoSn is around $3d^8$ and should not be very different in TiCoSb. The Co nuclear attraction is of course the same in both compounds; the intra-atomic correlations in the Co 3d shell have probably the same important magnitude, hence the electron transfer will be rather small, which prevents a complete filling of the shell. The gap found in TiCoSb is thus probably of the Mott–Hubbard type, related to the correlation energy U, and not a charge transfer gap.

Turning now to the resistivity behaviour, we noted that in the metallic state, the A

coefficient of the low-temperature quadratic variation $\rho(T) = \rho(0) + AT^2$ passes through a maximum value for $x = 0.6$, a concentration where T_C drops very rapidly.

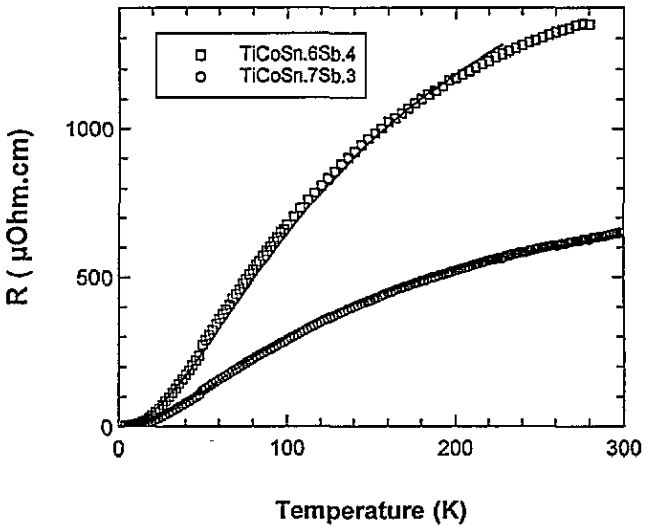

Figure 12. Magnetic contribution to the resistivity in $TiCoSn_{0.7}Sb_{0.3}$ and $TiCoSn_{0.6}Sb_{0.4}$. The continuous lines are fits to the spin fluctuation model of Rivier and Zlatic, with $T_{sf} = 240$ K and 280 K respectively.

This behaviour is characteristic of the crossover between ferromagnetic and paramagnetic regimes; the A coefficient can be then related to the fluctuation temperature T_{sf} [17, 18]. Again a comparison with $ZrZn_2$ shows that the A value for this compound is close to that for the solution with $x(\mathrm{Sn}) = 0.8$, which has a similar saturation moment of 0.15 μ_B.

Figure 1 shows that the resistivities for samples with $x = 1$, 0.9, 0.8 have a weaker temperature dependence, whereas those with $x = 0.7$, 0.6 and 0.5 exhibit a S-like shape and a larger negative curvature of the resistivity at high temperatures, together with the enhancement of the A coefficient. A flat resistivity is recovered for $x = 0.4$, when the ferromagnetism has disappeared. It is therefore interesting to compare the magnetic resistivity of these compounds to the results of spin fluctuation models; one analytic form of the resistivity is given for instance by Rivier and Zlatic [18]. We shall focus on the compounds which are close to magnetic instability, as the magnetic resistivity may be significantly reduced below the Curie point.

One problem is to find the phonon contribution, which cannot be given by the neighbouring non-magnetic compounds as they turn semiconducting. We thus used the resistivity of $TiNi_2Sn$, which has a Debye temperature $\Theta_D = 190$ K and seems to be representative of the phonon resistivity in TiCoSn. Band calculations [16] indeed show that the density of states in $TiNi_2Sn$ is slightly smaller than that for TiCoSn. Metallic TiNiSb also gives the same order of magnitude for the phonon resistivity, which is about 20 times less than the magnetic contribution in these magnetic samples. Subtracting such a phonon contribution gives the magnetic part drawn in figure 12 for $TiCoSn_{0.7}Sb_{0.3}$ and $TiCoSn_{0.6}Sb_{0.4}$; the corresponding fits according to [18] give spin fluctuation temperature $T_{sf} = 240$ K and 260 K respectively. These spin fluctuation temperatures are much higher than the observed Curie temperature, thus, according to Mohn and Wohlfarth [19], the Curie

temperature is mostly ruled by the Stoner model and slightly modified by the fluctuations. Indeed, the reduction in the density of states as the upper edge of the band is reached is obviously the leading factor for the disappearance of ferromagnetism.

6. Conclusion

The study of the TiCoSn–TiCoSb series showed the disappearance of ferromagnetism related to the lowering in the density of states when the metal–semiconductor transition is approached. It was shown that most probably an intermediate paramagnetic metallic phase exists, although a two-phase region blurs that part of the diagram. In the metallic regime, the general behaviour in this series is quite similar to that of the $ZrZn_2$ weak ferromagnet under pressure.

A comparison with the previously studied Co–Ni series allowed us to understand the different behaviours of itinerant magnetism in the case of a classical ferromagnetic to Pauli metal transition, or in the case of a ferromagnetic metal to non-magnetic semiconductor crossover. The difference from these previous studies is that we keep the same 3d electron number, while changing the sp element. It seems that the 3d shell is not filled in the final compound TiCoSb, but that probably an even number of 3d electrons from both Co and Ti stabilizes a non-magnetic configuration linked to a gap due to intraatomic correlations.

A new and interesting feature is the observation that the spontaneous Hall effect in TiCoSn does not vanish at the Curie point, due to short-range correlations in the paramagnetic state.

References

[1] Hamzic A, Asomoza R and Campbell I A 1981 *J. Phys. F: Met. Phys.* **11** 1441
[2] Kübler J, Williams A R and Sommers C B 1938 *Phys. Rev.* B **28** 1745
[3] Ziebeck K R A and Webster P J 1974 *J. Phys. Chem. Solids* **35** 1
[4] van Engen P G, Buschow K H J and Erman M 1983 *J. Magn. Magn. Mater.* **30** 374
de Groot R A and Buschow K H J 1986 *J. Magn. Magn. Mater.* **54–57** 1377
[5] Pierre J, Skolozdra R V and Stadnyk Yu V 1993 *J. Magn. Magn. Mater.* **128** 93
[6] Booth J G 1988 *Ferromagnetic Materials* vol 4, ed E P Wohlfarth and K H J Buschow (New York: Elsevier) p 279
Skolozdra R V, Stadnyk Yu V, Gorelenko Yu V and Terletskaya E E 1990 *Sov. Phys.–Solid State* **32** 1536
[7] Pierre J, Skolozdra R V, Gorelenko Yu K and Kouacou M A 1994 *J. Magn. Magn. Mater.* **134** 95–105
Pierre J, Skolozdra R V and Kouacou M A 1995 *Physica* B **206–207** 8440
[8] Aliev F G, Brandt N B, Moschalkov V V, Kozyrkov V V, Skolozdra R V and Belogorokhov A I 1989 Z. *Phys.* B **75** 167
[9] Ogawa S 1977 *Physica* B **91** 82
[10] Moriya T and Kawabata A 1973 *J. Phys. Soc. Japan* **34** 639
[11] Gschneidner K A Jr and Ikeda K 1983 *J. Magn. Magn. Mater.* **31–34** 265–8
Gschneidner K A Jr and Dhar S K 1984 *Springer Series in Solid-State Sciences* vol 54 (Berlin: Springer) p 177–82 and references therein
[12] Grosche F M, Pfleiderer C, McMullan G J, Lonzarich G G and Bernhoeft N R 1995 *Physica* B **206–207** 20
[13] Moriya T 1979 *J. Magn. Magn. Mater.* **14** 1
[14] Lonzarich G G and Taillefer L 1985 *J. Phys. C: Solid State Phys.* **18** 4339
[15] Rhodes P and Wohlfarth E P 1963 *Proc. R. Soc.* **273** 247
[16] Tobola J, Pierre J, Kaprzyk S, Skolozdra R V and Kouacou M A 1995 *J. Magn. Magn. Mater.* submitted
[17] Ueda K and Moriya T 1975 *J. Phys. Soc. Japan* **39** 605
[18] Rivier N and Zlatic V 1972 *J. Phys. F: Met. Phys.* **2** L87, L99
[19] Mohn P and Wohlfarth E P 1987 *J. Phys. F: Met. Phys.* **17** 2421